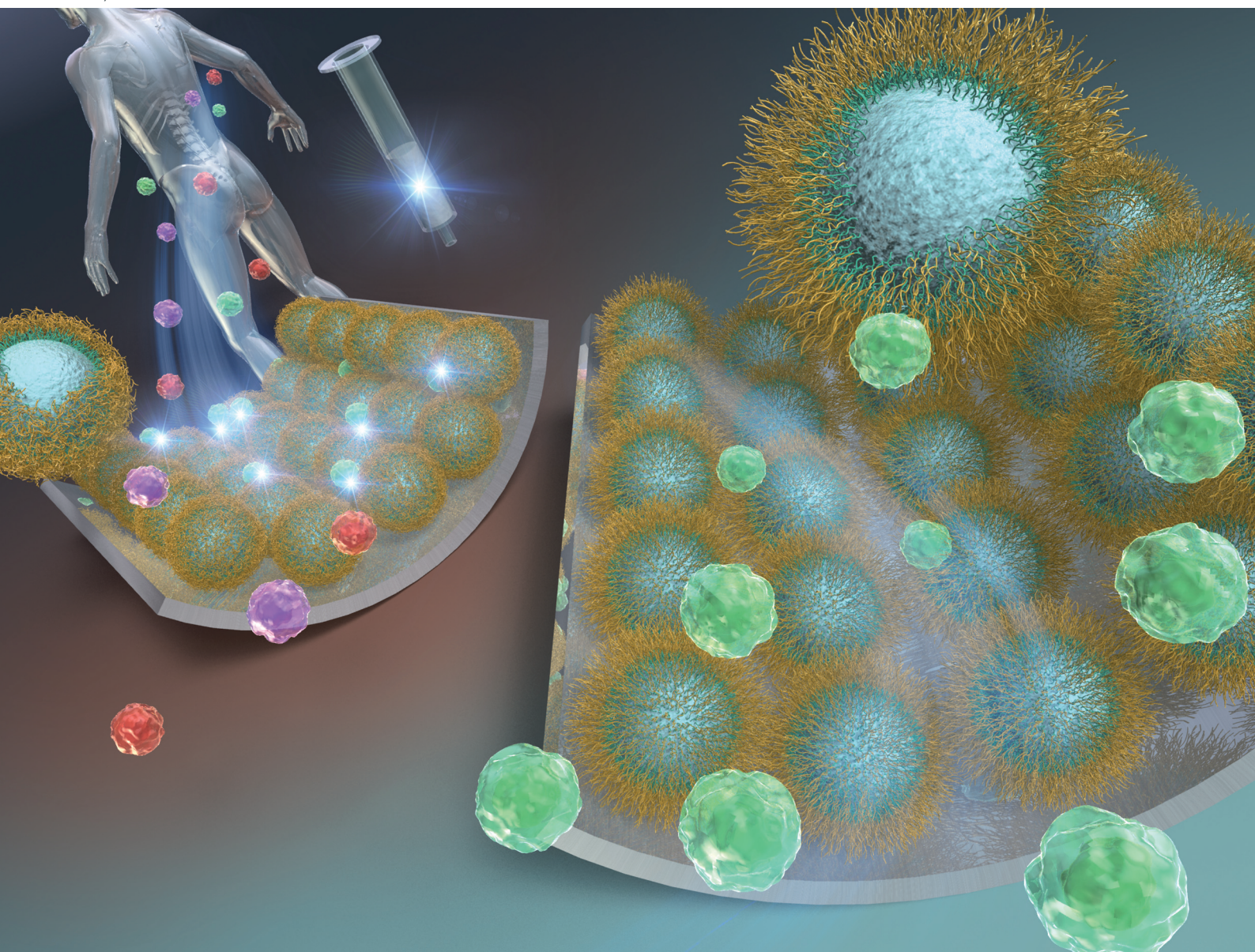


Biomaterials Science

Volume 9
Number 21
7 November 2021
Pages 6973-7312

rsc.li/biomaterials-science



ISSN 2047-4849



PAPER

Kenichi Nagase *et al.*

Thermally-modulated cell separation columns using a thermoresponsive block copolymer brush as a packing material for the purification of mesenchymal stem cells

Cite this: *Biomater. Sci.*, 2021, **9**, 7054

Thermally-modulated cell separation columns using a thermoresponsive block copolymer brush as a packing material for the purification of mesenchymal stem cells†

Kenichi Nagase, * Goro Edatsune, Yuki Nagata, Junnosuke Matsuda, Daiju Ichikawa, Sota Yamada, Yutaka Hattori and Hideko Kanazawa 

Cell therapy using mesenchymal stem cells (MSCs) is used as effective regenerative treatment. Cell therapy requires effective cell separation without cell modification and cellular activity reduction. In this study, we developed a temperature-modulated mesenchymal stem cell separation column. A temperature-responsive cationic block copolymer, poly(*N,N*-dimethylaminopropylacrylamide)-*b*-poly(*N*-isopropylacrylamide)(PDMAPAAm-*b*-PNIPAAm) brush with various cationic copolymer compositions, was grafted onto silica beads *via* two-step atom transfer radical polymerization. Using the packed beads, the elution behavior of the MSCs was observed. At 37 °C, the MSCs were adsorbed onto the column *via* both hydrophobic and electrostatic interactions with the PNIPAAm and PDMAPAAm segments of the copolymer brush, respectively. By reducing the temperature to 4 °C, the adsorbed MSCs were eluted from the column by reducing the hydrophobic and electrostatic interactions attributed to the hydration and extension of the PNIPAAm segment of the block copolymer brush. From the temperature-modulated adsorption and elution behavior of MSCs, a suitable PDMAPAAm composition of the block copolymer brush was determined. Using the column, a mixture of MSC and BM-CD34⁺ cells was separated by simply changing the column temperature. The column was used to purify the MSCs, with purities of 78.2%, *via* a temperature change from 37 °C to 4 °C. Additionally, the cellular activity of the MSCs was retained throughout the column separation step. Overall, the obtained results show that the developed column is useful for MSC separation without cell modification and cellular activity reduction.

Received 7th May 2021,
Accepted 5th July 2021

DOI: 10.1039/d1bm00708d

rsc.li/biomaterials-science

1. Introduction

Regenerative therapy by transplanting cell suspensions or cellular tissues into patients has become among the most effective cures for intractable diseases.^{1–6} In particular, regenerative therapy using mesenchymal stem cells (MSCs) has been attracting attention as an effective type of cell therapy.^{7–9} MSCs secrete various types of cytokines, leading to improve the function of damaged tissues.^{10–15} Furthermore, MSCs can be used in various types of stem cell based gene therapies.^{16,17}

In such types of therapy, cell separation is an essential protocol for the preparation of cell suspensions or the fabrication of cellular tissues, as MSCs are mixed with other types of cells in human bodily tissues. To date, various types of cell separ-

ation techniques have been developed.^{18–27} Among these, cell separation methods that include the modification of fluorescent-labeled antibodies or magnetic beads to cell surfaces have been widely used as precise cell separation techniques. However, the cell surface modification in separation techniques can reduce the intrinsic properties of cells, thus reducing their therapeutic effect. Therefore, cell separation techniques without the modification of cell surfaces are significantly for use in cell therapy applications.

Recently, cell separation using poly(*N*-isopropylacrylamide) (PNIPAAm) has been investigated as a technique that does not entail the modification of cell surfaces.^{28–34} PNIPAAm exhibits a temperature-dependent hydrophilic/hydrophobic property change attributed to hydration and dehydration, and PNIPAAm exhibits extension and shrinking. These unique properties of PNIPAAm are utilized in various types of biomedical applications, such as temperature-modulated drug delivery systems,^{35–38} PNIPAAm-conjugated proteins with temperature-modulated protein function changes,^{39–41} biosensing, bio-imaging system responses with external temperature

Faculty of Pharmacy, Keio University, 1-5-30 Shibakoen, MinatoTokyo 105-8512, Japan. E-mail: nagase-ki@pha.keio.ac.jp; Tel: +81-3-5400-1378; Fax: +81-3-5400-1378

†Electronic supplementary information (ESI) available. See DOI: 10.1039/d1bm00708d



changes,^{42–46} chromatographic separation systems using an all-aqueous mobile phase,^{47–49} and cell culture substrates for fabricating cellular tissues.^{50–54} In the cell separation systems that use PNIPAAm, cells are attached to PNIPAAm-modified glass surfaces at 37 °C, as the modified PNIPAAm on the glass becomes hydrophobic, and the cells tend to attach to the PNIPAAm surface. By reducing the temperature to 20 °C, the attached cells are detached from the surfaces, as the modified PNIPAAm becomes hydrophilic due to hydration, and the cells cannot attach to hydrophilic surfaces.

The differences in the attachment and detachment properties of the cells have been utilized for cell separation. For example, a mixture of myoblast and endothelial cells was separated using PNIPAAm-modified surfaces.²⁹ To increase the selectivity in the cell attachment, ionic PNIPAAm copolymer-modified surfaces were investigated. For example, using PNIPAAm copolymers with anionic groups, smooth muscle cells were separated from the endothelial cells.⁵⁵ Additionally, selective adhesion and detachment of the MSCs was performed using cationic PNIPAAm copolymer.^{56,57} In addition, micro/nano-imprinted substrates grafted with PNIPAAm were utilized to increase the difference in the cell adhesion properties among the fibroblasts, endothelial cells, and smooth muscle cells, leading to cell separation selectivity.³² These separation techniques can be used to separate cells by changing the temperature without modifying the cells. However, they use PNIPAAm copolymer-modified flat glass substrates or polymer film substrates, which have limited surface areas for cell attachment, leading to a limited amount of cell separation.

To overcome the above-mentioned problem, in this study, we developed a thermoresponsive cell separation column using PNIPAAm cationic block copolymer brush-modified beads as packing materials. Silica beads grafted with a block copolymer brush composed of cationic bottom segments and thermoresponsive upper segments were prepared *via* two-step surface-initiated atom transfer radical polymerization (ATRP). The cationic segment composition of the modified block copolymer brush was determined by observing the temperature-dependent cell elution behavior of the column. Using the bead packing column, the temperature-modulated separation of the MSCs from the bone marrow cells was simply performed by changing the temperature while maintaining the cellular activity without modification of the cell surfaces.

2. Materials and methods

2.1 Materials

N-Isopropylacrylamide (NIPAAm) and *N,N*-dimethylamino-propylacrylamide (DMAPAAm) were provided by KJ Chemicals (Tokyo, Japan), and NIPAAm was recrystallized from *n*-hexane. DMAPAAm was purified by distillation. Tris(2-aminoethyl) amine, formaldehyde, formic acid, sodium hydroxide, dichloromethane, magnesium sulfate, hydrochloride, acetone, 2-propanol, and copper(I) chloride were obtained from Fujifilm

Wako Pure Chemical Corporation (Osaka, Japan). α -Chloro-*p*-xylene was obtained from Tokyo Chemical Industries (Tokyo, Japan), and [(Chloromethyl)phenylethyl] trimethoxysilane (CPTMS) was obtained from Gelest (Morrisville, PA, USA). Tris [[2-dimethylamino)ethyl]amine (Me₆TREN) was synthesized from TREN.⁵⁸ Silica beads (Wakosil® C-200, pore diameter: 6 nm, surface area: 475 m² g⁻¹) were obtained from Fujifilm Wako Pure Chemical Corporation (Osaka, Japan). Porous silica beads were used in the present study because they are primarily used in sample preparation in chromatography and their modification conditions were easily determined from previous reports.^{59–62} An Extract-clean empty column was obtained from Systech (Tokyo, Japan), and MSCs were obtained from the JCRB cell bank (Osaka, Japan) and Promocell (Heidelberg, Germany). Bone marrow CD34⁺ cells (BM-CD34⁺) and normal human dermal fibroblasts (NHDFs) were obtained from Lonza (Basel, Switzerland), and Jurkat was obtained from the ATCC cell bank (Manassas, VA, USA). Cell culture media were obtained from Thermo Fisher Scientific (Waltham, MA, USA).

2.2 Preparation of the thermoresponsive cationic block copolymer brush

A thermoresponsive cationic block copolymer brush with various DMAPAAm compositions was prepared using two-step ATRP (Fig. 1A). Silica beads (64–210 μ m) were sieved to the fractions of 75–106 μ m, 106–150 μ m, and 150–210 μ m using sieves with 106 and 150 μ m meshes. Then, 50 g of the sieved beads of each fraction were washed with hydrochloride at 90 °C for 3 h. Then, the beads were filtered, rinsed with pure water, and then with acetone, respectively. Afterward, they were dried at 150 °C for 7 h using a drying vacuum oven (DP200, Yamato, Tokyo).

An ATRP initiator, CPTMS, was immobilized *via* a silane coupling reaction (Fig. 1A). The beads (10 g) were put in a 500 mL flask and humidified at a relative humidity of 60% for 3 h by flowing humidified nitrogen gas in the flask. Then, CPTMS (12.4 mL, 0.05 mol) was dissolved into 300 mL of toluene, and the CPTMS solution was poured into the flask. The silane coupling reaction was subsequently started at 25 °C for 16 h with continuous stirring. After the reaction, the silica beads were filtered and rinsed with acetone. Then, they were dried at 110 °C for 3 h in a vacuum oven.

PDMAPAAm was modified on the silica beads *via* the first ATRP process. The amount of PDMAPAAm on the silica beads was modulated by the amount of the DMAPAAm monomer in the ATRP reaction from 0.103 to 4.10 mmol. In the case of the polymerization of 0.103 mmol of DMAPAAm, DMAPAAm (15.9 mg, 0.103 mmol) were dissolved in 40 mL of 2-propanol in a 100 mL flask. The solution was deoxygenated by argon gas bubbling for 20 min. CuCl (26.22 mg, 0.26 mmol) and Me₆TREN (68.00 mg, 0.30 mmol) were dissolved in the solution under an argon gas atmosphere. Then, the flask was sealed and placed in a glove bag. CPTMS immobilized silica beads (3.0 g) were put into a 50 mL glass vessel, which was then placed in the same glove bag. The oxygen in the glove bag was removed by cycling between a vacuum and argon gas three



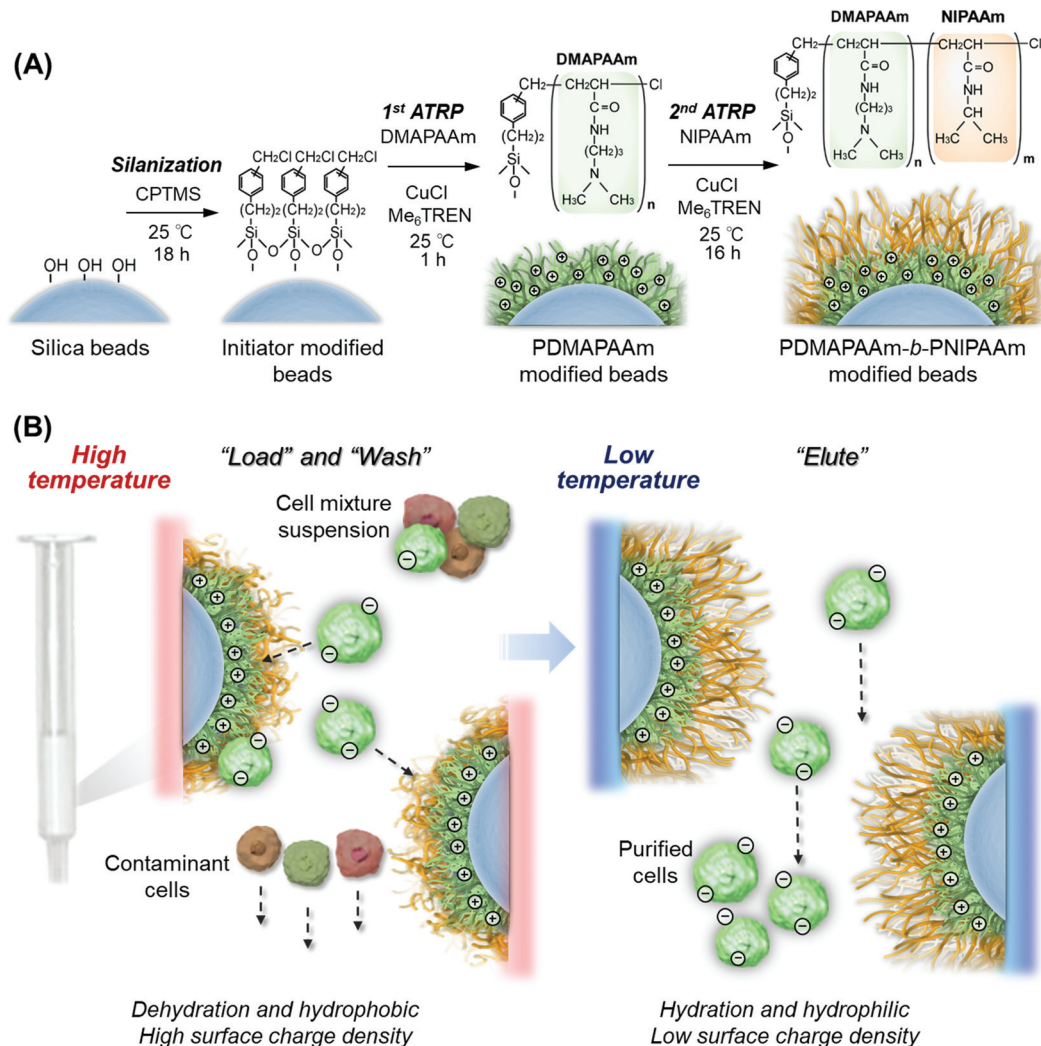


Fig. 1 Schematic illustration of (A) the preparation of the thermoresponsive cationic copolymer brush as a column packing material. (B) Column separation of MSCs using the bead packed column.

times. Then, the ATRP reaction solution was poured onto the silica beads in the glass vessel, and α -chloro-*p*-xylene (1.75 μ L, 1.32×10^{-5} mol) was added to the reaction solution. The glass vessel was sealed in the glove bag, and the reaction proceeded at 25 °C for 1 h with continuous shaking. After the reaction, the silica beads were filtered and rinsed with acetone, and the beads were dried at 50 °C for 3 h in a vacuum oven.

PDMAPAAm-*b*-PNIPAAm-grafted silica beads were prepared *via* the second ATRP reaction for the block copolymerization of NIPAAm from the PDMAPAAm-grafted silica beads. NIPAAm (4.60 g, 40.7 mmol) were dissolved in 40 mL of 2-propanol in a 100 mL flask, and the solution was deoxygenated by argon gas bubbling for 20 min. CuCl (26.22 mg, 0.26 mmol) and Me₆TREN (68.00 mg, 0.30 mmol) were dissolved in the solution under argon gas. Then, the flask was sealed and placed in a glove bag. PDMAPAAm-grafted silica beads (2.8 g) were put in a 50 mL glass vessel, which was then placed in the same glove bag. The oxygen in the glove bag was removed by cycling

between a vacuum argon gas three times. Then, the ATRP reaction solution was poured onto the silica beads in the glass vessel, and α -chloro-*p*-xylene (1.75 μ L, 1.32×10^{-5} mol) was added to the reaction solution. The glass vessel was sealed in the glove bag, and the reaction proceeded at 25 °C for 16 h with continuous shaking. After the reaction, the silica beads were filtered and rinsed with acetone, and the beads were washed with a mixture solution of 50 mM EDTA and methanol (1 : 1) with sonification. Then, the beads were filtered, rinsed with pure water, and dried at 50 °C for 3 h in a vacuum oven.

For comparison, PNIPAAm homopolymer modified silica beads were prepared *via* the same ATRP procedure as in the second ATRP reaction, except that CPTMS-modified beads were used in place of PDMAPAAm-modified beads.

The prepared beads were named as PDX-*b*-PN, where *X* is the molar percentage of DMAPAAm to NIPAAm in the ATRP reaction.



2.3 Characterization of the thermoresponsive cationic block copolymer brush

The prepared polymer-modified silica beads were characterized *via* carbon/hydrogen/nitrogen (CHN) elemental analysis, attenuated total reflection/Fourier-transform infrared spectroscopy (ATR/FTIR), and field-emission scanning electron microscopy (FE-SEM).

The carbon composition of the prepared beads was measured using a CHN elemental analyzer (PE2400, PerkinElmer, Waltham, MA, USA). The amount of initiator and polymer on the silica beads was estimated from the carbon composition of the beads, and the amount of the immobilized initiator on the silica beads was estimated as follows:

$$\frac{\%C_I}{\%C_I(\text{calcd}) \times (1 - \%C_I/\%C_I(\text{calcd}))} \times S', \quad (1)$$

where $\%C_I$ is the increase in the carbon percentage of the initiator-modified beads through the silane coupling reaction, $\%C_I(\text{calcd})$ is the calculated percentage of carbon in the CPTMS, and S' is the surface area of the beads ($475 \text{ m}^2 \text{ g}^{-1}$). The amount of PDMAAm was obtained using the following equation:

$$\frac{\%C_D}{\%C_D(\text{calcd}) \times (1 - \%C_D/\%C_D(\text{calcd}) - \%C_I/\%C_I(\text{calcd}))} \times S', \quad (2)$$

where $\%C_D$ is the increase in the percentage of carbon in the PDMAAm-modified beads after the first ATRP process, and $\%C_D(\text{calcd})$ is the calculated percentage of carbon in DMAAm. The amount of the modified PNIPAAm segments after the second ATRP process was estimated as follows:

$$\frac{\%C_N}{\%C_N(\text{calcd}) \times (1 - \%C_N/\%C_N(\text{calcd}) - \%C_D/\%C_D(\text{calcd}) - \%C_I/\%C_I(\text{calcd}))} \times S', \quad (3)$$

where $\%C_N$ is the increase in the percentage of carbon in the PDMAAm-*b*-PNIPAAm-modified beads after the second ATRP process, and $\%C_N(\text{calcd})$ is the calculated percentage of carbon in NIPAAm. The amount of modified block copolymer was obtained by summing the amounts of PDMAAm (eqn (2)) and PNIPAAm (eqn (3)).

The polymer modification of the silica beads after each ATRP process was confirmed by ATR/FTIR using a FTIR-4700 spectrometer (JASCO, Tokyo, Japan).

The surface morphology of the beads was observed by FE-SEM using an S-4700 microscope (Hitachi High Technologies, Tokyo, Japan).

2.4 Cell elution from the bead packed column

The beads were packed into an empty solid-phase extraction column (inner diameter: 0.9 mm, length: 65 mm, total volume: 1.5 mL). A filter with 50 μm mesh was placed in the column, and the prepared beads (300 mg) were added afterward. A small amount of a solvent mixture of water : methanol = 1 : 1 was added to dampen the packed beads. Then, the filter was placed on the packed beads in the column. The packed

column was rinsed with a solvent mixture of water : methanol = 1 : 1, ethanol, and pure water.

The cells were cultured using the cell culture medium shown in Table S1.† Before loading the cell suspension onto the column, 5 mL of the cell culture medium, which was warmed at 37 °C, was flowed through the column. Then, 1 mL of cell suspension (5.0×10^5 cells per mL) was passed through a cell strainer, and the cell suspension was introduced onto the column at a flow rate of 1 mL min^{-1} using a syringe pump (YSP-202, YMC, Kyoto, Japan) while maintaining the column temperature at 37 °C using a column temperature controller (Senshu Scientific, Tokyo, Japan). The eluted fraction from the column was defined as the “Load.” Then, the cell culture medium (1 mL) was flowed through the column at 37 °C at a flow rate of 1 mL min^{-1} so as to rinse the nonadsorbed cells from the column. The flowing process was performed two times. Each eluted fraction was defined as the “Wash.” Then, the column was cooled at 4 °C, and 1 mL of the cell culture medium, which was cooled at 4 °C, was flowed into the column using a syringe pump at a flow rate of 9 mL min^{-1} . The flowing process was performed three times. Each eluted fraction was defined as the “Elute,” and the amount of cells in each fraction was measured using a cell viability analyzer (Vi-CELL XR, Beckman Coulter, Pasadena, CA, USA). The cell recovery ratio was obtained from the ratio of eluted cells to loaded cells.

A cell separation experiment was performed using a similar procedure. A mixture of MSCs and BM-CD34⁺ cells was prepared by mixing each cell suspension at a cell density of 5.0×10^5 cells per mL. The cell suspension (1 mL) was flowed through the column at 37 °C at a flow rate of 1 mL min^{-1} , and

the eluted fraction was defined as the “Load” fraction. Then, the cell culture medium (1 mL) was flowed through the column at 37 °C at a flow rate of 1 mL min^{-1} , and this process was repeated four times. Each eluted fraction was mixed, and the mixed fraction was defined as the “Wash.” Then, 1 mL of the cooled cell culture medium was flowed through the column, and the adsorbed cells were eluted. Elution was then performed five times. The eluted fraction was mixed, and the mixed fraction was defined as the “Elute.” The cell composition of each fraction was measured through flow cytometry with the modification of the MSCs with CD73-PE antibodies.

The cell viability of the eluted fraction was observed using a trypan blue exclusion test with a cell viability analyzer (Vi-CELL XR). The viability of cells before the column loading was also observed as a control.

The cell proliferation ability of the recovered MSCs from the column was investigated by culturing the cells in a 24-well cell culture plate with a predetermined culture period of four days. Then, the cells were recovered with trypsin and were counted using a cell viability analyzer (Vi-CELL XR). The cells before the column loading were cultured and used as a control.



The differentiation ability of the recovered MSCs from the column was evaluated using osteogenic and adipogenic differentiations. The osteogenic differentiation of the MSCs was performed by culturing them with an osteogenic differentiation medium for 9 days, where the medium was replaced every four days. The osteogenic differentiation was confirmed through alizarin red staining. The adipogenic differentiation of the MSCs was performed by culturing them with an adipogenic differentiation medium for 12 days, where the medium was replaced every four days. The adipogenic differentiation was confirmed by oil red O staining.

3. Results and discussion

3.1 Characterization of the thermoresponsive cationic block copolymer brush on the silica beads

PDMAPAAm-*b*-PNIPAAm brush-modified beads were prepared *via* two-step surface-initiated ATRP. The prepared beads were characterized using a CHN elemental analysis to estimate the amount of the immobilized initiator and polymer on the silica beads (Table 1). A higher carbon composition was observed on the initiator-immobilized silica beads than on the unmodified silica beads, as the CPTMS was immobilized on the silica beads *via* a silane coupling reaction. The amount of immobilized CPTMS was $2.99 \mu\text{mol m}^{-2}$, which is almost the same as the silanol group density on the silica bead surface.⁶³ These results indicate that most of the silanol groups on the silica beads were used for the coupling reaction with CPTMS. The carbon and nitrogen compositions of the PDMAPAAm-modified silica beads (PD0.25, PD0.5, PD1, and PD10) exhibited a higher carbon composition compared with the initiator-immobilized silica beads, indicating that PDMAPAAm was modified during the first step of the ATRP reaction. The amount of the modified PDMAPAAm increased with an increase in the DMAPAAm monomer in the first ATRP reaction, as this increase enhanced the polymerization rate, leading to an increase in the amount of modified PDMAPAAm on the silica beads. Higher carbon and nitrogen compositions

were observed on the PDMAPAAm-*b*-PNIPAAm-modified silica beads compared with the PDMAPAAm-modified silica beads, indicating that during the second ATRP reaction PNIPAAm segments were successfully grafted on PDMAPAAm. The amount of modified block copolymer, PDMAPAAm-*b*-PNIPAAm, was relatively small compared with the previously reported polymer brush-modified silica beads due to the small pore diameter of the beads (6 nm).^{64,65} In the previous study, silica beads with a pore diameter of 30 nm were used. Thus, the polymers were grafted inside the pores of the beads through surface-initiated polymerization.^{66,67} However, the pore diameter of the silica beads in this study is small. Thus, effective copolymer grafting inside the pores was not performed, whereas copolymer modification on the outer surfaces of the beads was performed, leading to a relatively smaller grafted amount of copolymer on the silica beads. However, in this study, the copolymer-grafted silica beads were used as a packing material in the cell separation column. Thus, copolymer modification inside the pores was not required as the cells cannot enter inside them.

Polymer modification *via* ATRP was also confirmed by observing the FTIR spectra (Fig. 2). Two additional peaks were observed at approximately 1550 and 1645 cm^{-1} in the FTIR spectra of the PNIPAAm-modified, PDMAPAAm-modified, and PDMAPAAm-*b*-PNIPAAm-modified beads. These peaks were attributed to the C=O stretching and N-H bending vibrations of the amide groups of DMAPAAm and NIPAAm. Thus, these results indicate that polymer modification was successfully performed *via* ATRP.

SEM observations of the prepared silica beads were performed after each reaction step to confirm the morphology of the silica beads (Fig. 3). The silica beads maintained their spherical morphology after the silane coupling reaction and the first and second ATRP reactions. These results indicate that the reaction steps did not deform the silica beads.

3.2 Cell elution behavior using the bead packed column

The prepared beads were packed into a syringe-type column. The cell elution behavior was observed using MSCs. At first,

Table 1 Characterization of the prepared thermoresponsive cationic block copolymer-modified beads

Code ^a	Elemental composition ^b (%)			Immobilized initiator ^c ($\mu\text{mol m}^{-2}$)	Grafted polymer ^c (mg m^{-2})
	C	H	N		
Unmodified silica beads	0.21 ± 0.03	0.64 ± 0.31	0.04 ± 0.03		
Initiator-immobilized silica beads	12.19 ± 0.16	0.67 ± 0.04	0.02 ± 0.01	2.99	
PN	16.75 ± 0.82	1.47 ± 0.17	1.40 ± 0.08		0.208
PD0.25	12.51 ± 0.07	0.92 ± 0.06	0.42 ± 0.00		0.014
PDN0.25- <i>b</i> -PN	17.68 ± 0.33	1.69 ± 0.06	1.60 ± 0.02		0.257
PD0.5	12.89 ± 0.16	0.94 ± 0.11	0.39 ± 0.02		0.030
PD0.5- <i>b</i> -PN	17.05 ± 0.34	1.46 ± 0.05	1.43 ± 0.04		0.225
PD1	13.00 ± 0.09	0.93 ± 0.09	0.44 ± 0.02		0.035
PD1- <i>b</i> -PN	17.46 ± 0.07	1.45 ± 0.05	1.39 ± 0.03		0.247
PD10	14.33 ± 0.15	1.05 ± 0.03	1.02 ± 0.01		0.096
PD10- <i>b</i> -PN	18.39 ± 0.77	1.68 ± 0.13	1.89 ± 0.07		0.299

^a The code of the prepared thermoresponsive copolymer brush-modified beads was determined as "PD*X*-*b*-PN", where *X* is the molar percentage of DMAPAAm to that of NIPAAm in ATRP. ^b Determined by the CHN elemental analysis. ^c Estimated using the carbon composition.



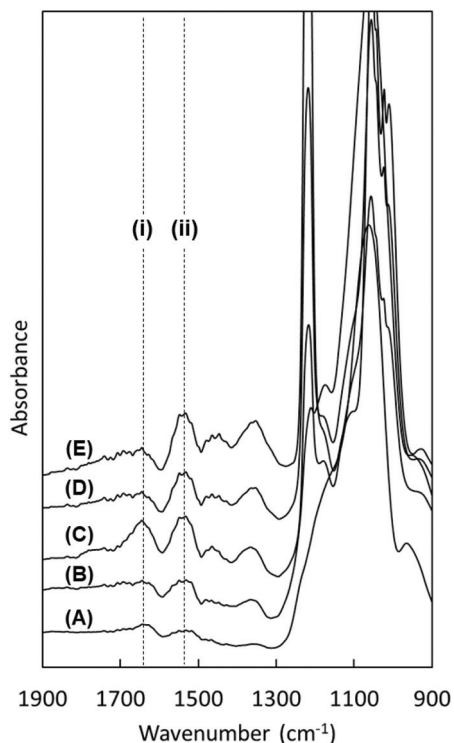


Fig. 2 Fourier-transform infrared spectroscopy (FTIR) spectra of the prepared beads. (A) Unmodified silica beads, (B) initiator-modified silica beads, (C) PNIPAAm-modified beads (PN), (D) PDMAPAAm-modified silica beads (PD0.5), and (E) PDMAPAAm-*b*-PNIPAAm-modified beads (PD0.5-*b*-PN). Lines (i) and (ii) represent the peaks attributed to C=O stretching and N–H bending vibrations, respectively.

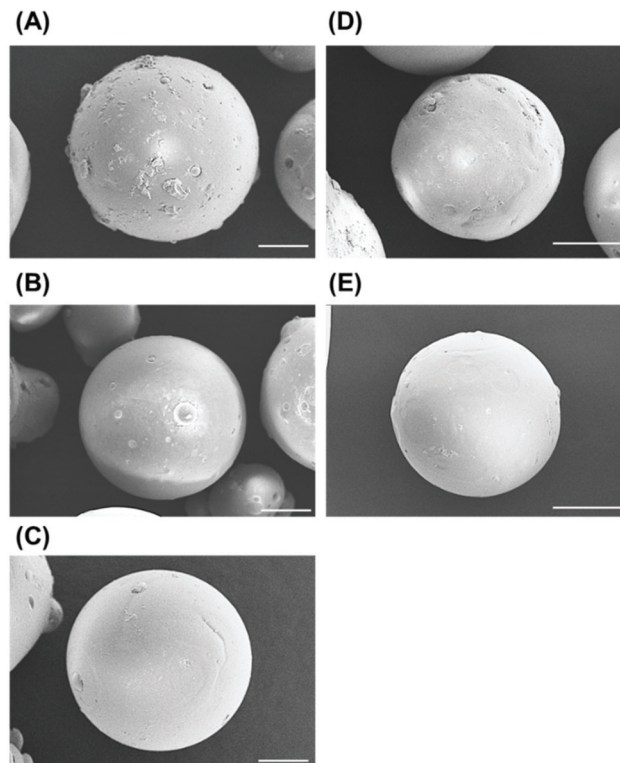


Fig. 3 Field-emission scanning electron microscopy (FE-SEM) images of the prepared beads. (A) Unmodified beads, (B) initiator-modified beads, (C) PNIPAAm-modified beads (PN), (D) PDMAPAAm-modified silica beads (PD0.5), and (E) PDMAPAAm-*b*-PNIPAAm-modified beads (PD0.5-*b*-PN). Scale bars: 50 μm .

the proper bead size was investigated using two types of bead fractions as packing materials for the column. Two types of PNIPAAm-modified silica beads with diameters of 106–150 and 150–210 μm were used as packing materials, and the elution behavior of the MSCs was observed (Fig. 4). Both columns exhibited temperature-dependent cell elution. Greater cell elution was observed in the elute fraction at 4 $^{\circ}\text{C}$ compared with the load and wash fractions at 37 $^{\circ}\text{C}$ because of the temperature-modulated cell adsorption and desorption, which are attributed to the hydrophobicity change of PNIPAAm. In the wash and elute fractions at 37 $^{\circ}\text{C}$, the bead surface became hydrophobic due to the dehydration of the modified PNIPAAm, leading to cell adsorption on the beads. On the contrary, at 4 $^{\circ}\text{C}$, the PNIPAAm on the beads became hydrophilic, and the adsorbed cells were detached from the bead surface, leading to the elution of the cells from the column. Greater elution was observed on the 150–210 μm bead packed column compared with the 106–150 μm bead packed column, which is due to the gaps of the packed beads in the column. The cells were flowed through the gaps of the packed beads in the column. In the case of the 106–150 μm beads packed column, the gaps were not adequate to allow cells to flow through. Thus, a quite low cell elution ratio was observed on the 106–150 μm bead packed column. These results indi-

cate that the 150–210 μm beads are more suitable as column packing materials than the 106–150 μm beads.

To investigate the proper cationic composition of the modified copolymers, the MSC elution behavior was observed on columns with various PDMAPAAm compositions (Fig. 5). On all the columns, MSCs were adsorbed at 37 $^{\circ}\text{C}$ and eluted at 4 $^{\circ}\text{C}$ because the temperature-responsive properties of the PDMAPAAm-*b*-PNIPAAm brush on the silica beads changes. At 37 $^{\circ}\text{C}$, the upper PNIPAAm segment in the block copolymer became hydrophobic due to dehydration, leading to the adsorption of MSCs on the copolymer. Also, the upper PNIPAAm segment was shrunk, and the cationic bottom PDMAPAAm layer was exposed, leading to enhanced cell adsorption through electrostatic interactions attributed to the negatively-charged MSCs, the zeta potential of which is -24.5 mV (Table S2 †). These factors enhanced the cell adsorption on the copolymer brush at 37 $^{\circ}\text{C}$. On the contrary, at 4 $^{\circ}\text{C}$, the PNIPAAm segment in the block copolymer became hydrophilic due to hydration. Also, the PNIPAAm segment was extended, leading to the prevention of electrostatic interactions between the bottom PDMAPAAm segment of the block copolymer and the cells. These factors led to the detachment of the MSCs from the copolymer brush.



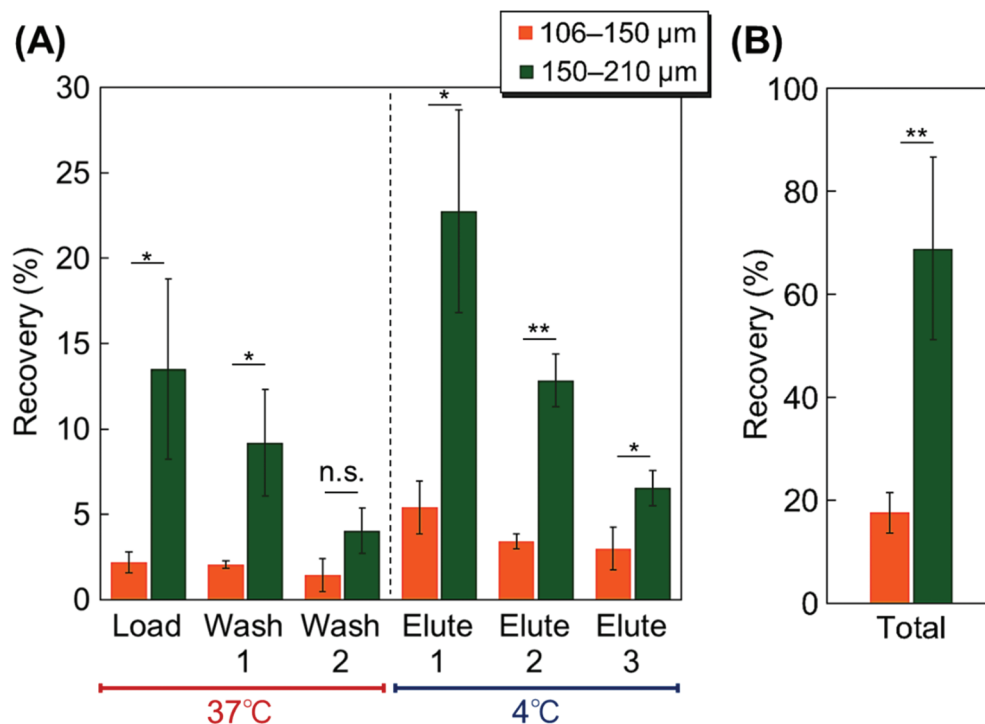


Fig. 4 Elution behavior of the MSCs from the columns using two types of beads grafted with PNIPAAm ($n = 3$). (A) Elution behavior of each fraction. (B) Total recovery ratio of the MSCs from the column. (*: $P < 0.05$; **: $P < 0.01$; and n.s.: not significant).

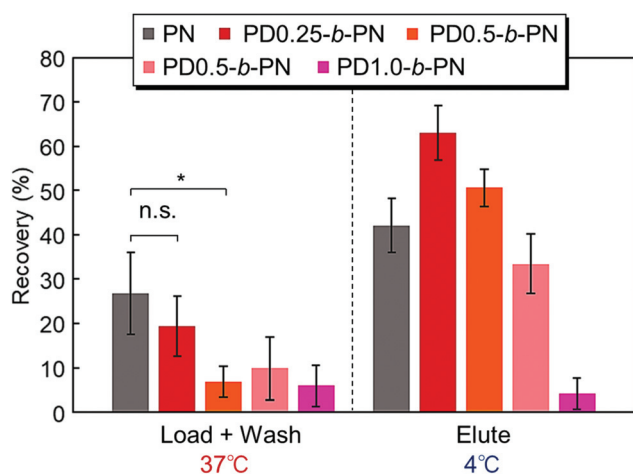


Fig. 5 Recovery ratio of the MSCs from columns using various cationic copolymer composition-modified silica beads as packing materials ($n = 3$). (*: $P < 0.05$ and n.s.: not significant).

A previous report indicated that the PDMAPAm-*b*-PNIPAAm brush-modified glass substrate can be used to perform temperature-modulated selective adhesion and detachment of umbilical cord derived MSCs (UC-MSCs).⁵⁷ UC-MSCs interact with PDMAPAAm-*b*-PNIPAAm brush grafted glass cover slips at 37 °C because of the electrostatic interaction between the MSCs and bottom PDMAPAAm segment. Additionally, the

PNIPAAm segment in block copolymer brush became hydrophobic, leading to enhanced adhesion of the MSCs on copolymer brush. By reducing the temperature, the PNIPAAm segment in the block copolymer brush became hydrated and extended, leading to the selective detachment of the UC-MSCs.⁵⁷ In the present study, bone marrow derived MSCs also adsorbed to PDMAPAAm-*b*-PNIPAAm brush on the silica beads in the same manner, although there was a difference between the bone marrow derived MSCs and UC-MSCs.

At 37 °C, during the load and wash fractions, the MSC adsorption was enhanced with an increase in the PDMAPAAm composition on the beads. In addition, at 4 °C, in the elute fractions, the recovery ratio decreased with an increase in the PDMAPAAm composition due to the enhanced electrostatic interactions between the MSCs and copolymer brush. Thus, the electrostatic interactions between the cationic PDMAPAAm segment and MSCs increased with an increase in the PDMAPAAm amount in the copolymer segment. Among all the columns, PD0.5-*b*-PN exhibited effective MSC adsorption at 37 °C and elution at 4 °C.

The viability of the eluted MSCs from the various PDMAPAAm composition columns was observed using a trypan blue exclusion test (Fig. 6). The viability of the eluted MSCs decreased with an increase in the PDMAPAAm composition. In particular, PD1.0-*b*-PN and PD10-*b*-PN exhibited low viability. The cationic properties of the copolymer-modified beads led to an interaction with cell membrane proteins, and changes in the three-dimensional structure of the cell surface



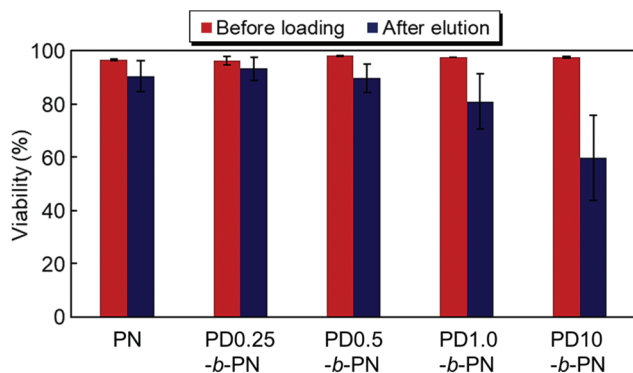


Fig. 6 Cell viability of the MSCs before loading and after elution from the columns with various cationic compositions of the copolymer.

membrane proteins. Thus, strong cationic properties, such as those of PD1.0-*b*-PN and PD10-*b*-PN, disrupted the cell membrane, leading to eluted MSCs with low viability. On the contrary, PD0.25-*b*-PN and PD0.5-*b*-PN exhibited retained cell viability, indicating that the relatively weak cationic properties of the beads retained the structure of the cell membrane. Thus, the PDMAPAAm composition was suitable below PD1.0-*b*-PN. The cell adhesion behavior of the eluted MSCs from PN and PD0.5-*b*-PN on the tissue culture polystyrene dish was observed (Fig. S1†). The MSCs from the eluted column exhibited a similar cell adhesion behavior to that before column loading. These results show that PN and PD0.5-*b*-PN maintained cell activity when passed through the column.

Considering the elution behavior of the MSCs from the column and cell viability, the most suitable column material for temperature-modulated MSC adsorption and detachment is PD0.5-*b*-PN.

Using the PD0.5-*b*-PN column, the elution behavior of BM-CD34⁺, NHDFs, and Jurkat cells was observed and then compared with that of the MSCs (Fig. 7). BM-CD34⁺ is derived from the bone marrow and then used as a model of contaminant cells in the bone marrow with the MSCs. NHDF was used as a model of adhesive cells, and Jurkat was used as a model of floating cells. The zeta potentials of these cells were

measured (Table S2†). BM-CD34⁺ and Jurkat exhibited large cell elution at 37 °C, indicating that the cells were not adsorbed on the block copolymer brush at 37 °C. On the contrary, MSCs were adsorbed on the copolymer brush at 37 °C, leading to the low elution of the MSCs at 37 °C. This is probably due to the difference in the negative charges of the cells. The zeta potentials of BM-CD34⁺ and Jurkat were -6.70 and -2.5, respectively. On the contrary, the zeta potential of the MSCs was -24.5 mV. Thus, the MSCs were adsorbed on the copolymer brush *via* relatively strong electrostatic interactions compared with the BM-CD34⁺ and Jurkat cells. NHDF exhibited a low elution ratio at both 37 °C and 4 °C, which is probably due to the intrinsic adhesive properties of the NHDFs. The NHDFs exhibited strong adhesive properties on the PNIPAAm-modified interfaces compared with the other types of cells.^{30,32,57} These properties led to strong adsorption of the NHDFs on the column at both 37 °C and 4 °C.

To investigate the cell separation efficiency of the column, the elution behavior of a mixture of MSCs and BM-CD34⁺ cells was observed using the PD0.5-*b*-PN column (Fig. 8). The same amounts of MSCs and BM-CD34⁺ cells were mixed together, and a mixed cell suspension was introduced onto the column. At 37 °C, the load and wash fractions contained a large composition of BM-CD34⁺ cells and barely contained MSCs, as the electrostatic interactions between the copolymer and BM-CD34⁺ cells was relatively low compared with that of the MSCs. By reducing the temperature to 4 °C, the elute fraction contained a large composition of MSCs, as the adsorbed MSCs on the copolymer brush were detached due to the hydration and extension of the PNIPAAm segment of the copolymer after lowering the temperature, leading to the elution of the MSCs from the column. This result indicates that the developed PD0.5-*b*-PN column separated the MSCs and other contaminant cells in the bone marrow by simply changing the column temperature. The purity of the MSCs is approximately 80%, which is not relatively high compared to that of the purification of MSCs through fluorescent-activated cell sorting (FACS) and magnetic-activated cell sorting (MACS). However, the developed temperature-responsive cell separation column can purify the MSCs without modifying the cell surfaces,

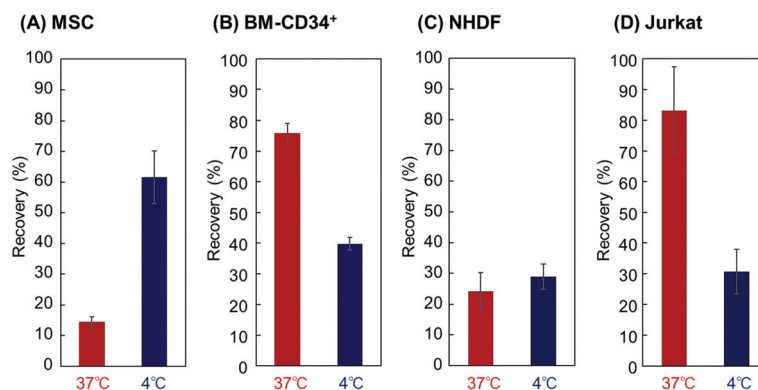


Fig. 7 Cell recovery ratio through the PD0.5-*b*-PN column using (A) MSCs, and (B) BM-CD34⁺, (C) NHDFs, and (D) Jurkat cells.



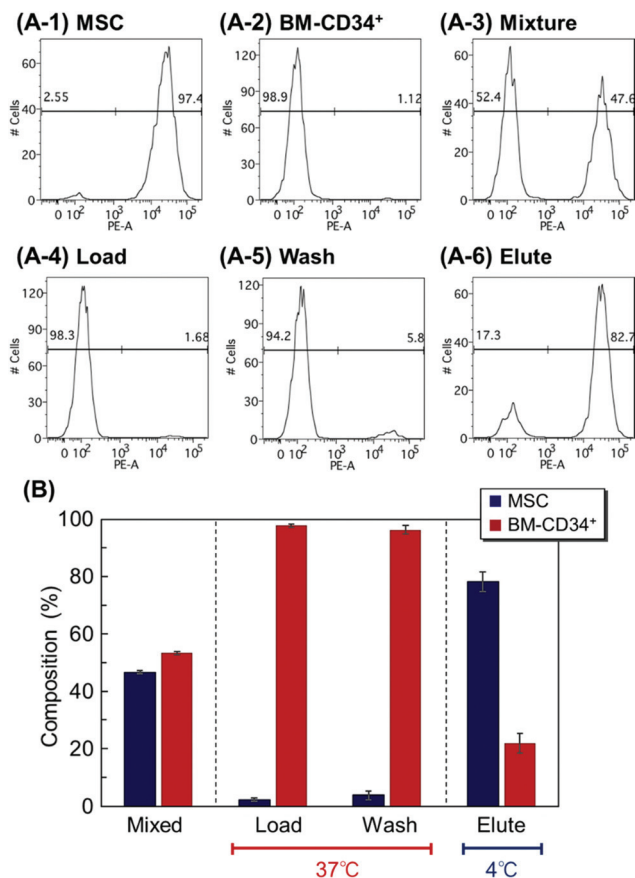


Fig. 8 Cell separation using the PD0.5-*b*-PN column by applying a mixture of MSCs and CD-34⁺ cells. (A) Representative data of the flow cytometry analysis of each fraction. (A-1) MSCs, (A-2) BM-CD34⁺ cells, (A-3) cell mixture of MSCs and BM-CD34⁺ cells, (A-4) load fraction at 37 °C, (A-5) wash fraction at 37 °C, and (A-6) elution fraction at 4 °C. (B) Cell composition of each fraction through the PD0.5-*b*-PN column.

which is an advantage for the utilization of purified MSCs for cell transplantation therapy. This is because the cell modification process in FACS or MACS would lose the cell's intrinsic properties leading to reduced cell therapeutic effect after transplantation.

The cell proliferation and differentiation of the recovered MSCs from the column were observed (Fig. S2† and Fig. 9) to investigate their cellular activities. The recovered MSCs from the PD0.5-*b*-PN column in the elute fraction were seeded and cultured on a cell culture dish, and the cell number at the pre-determined culture period was observed. The recovered MSCs from the column exhibited a similar proliferation ability to those without column loading (Fig. S2†). Also, the differentiation ability of the recovered MSCs from the column was investigated through osteogenic and adipogenic differentiations of the MSCs (Fig. 9). The recovered MSCs from the PD0.5-*b*-PN column in the elution fraction were differentiated by culturing them with the osteogenic and adipogenic differentiation media. The alizarin red S staining of the osteogenic-differentiated MSCs indicated that the recovered MSCs could be differentiated to osteoblasts, similar to the control MSCs, which were not passed through the column (Fig. 9). In addition, osteocalcin was observed in the MSCs after osteogenic differentiation (Fig. S3†). Additionally, the oil red O staining in the adipogenic-differentiated MSCs exhibited similar adipogenic differentiation to the control MSCs, which were not passed through the column. These results indicate that the recovered MSCs from the column maintained their proliferation and differentiation abilities.

Overall, the developed thermoresponsive cationic block copolymer brush-modified bead packed column in this study modulated MSC adsorption and elution by changing the surface hydrophobicity of the beads and the electrostatic interactions between the copolymers and cells. Using these pro-

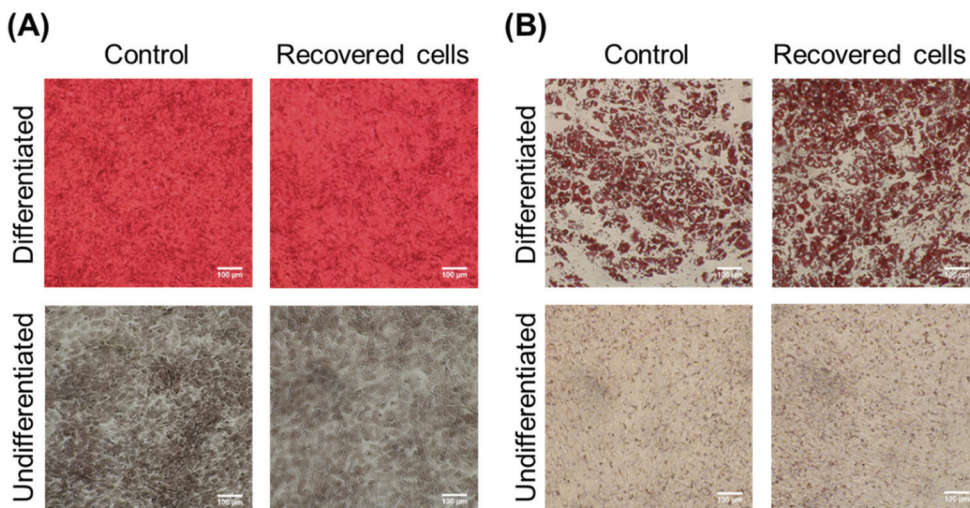


Fig. 9 Evaluation of the differentiation potency of the recovered cells by (A) the osteogenic differentiation of MSCs *via* alizarin red S staining and (B) the adipogenic differentiation of the MSCs with oil red O staining. Scale bar: 100 μ m.



properties, MSCs can be simply separated by changing the temperature while maintaining cellular activities, such as viability, proliferation ability, *etc.* Thus, the developed columns in this study are useful cell separation tools for MSCs.

4. Conclusions

In this study, we developed temperature-modulated MSC separation columns using thermoresponsive cationic block copolymer brush-modified beads as packing materials. A thermoresponsive cationic block copolymer, PDMAPAAm-*b*-PNIPAAm brush, was prepared on silica beads *via* a two-step ATRP reaction. At 37 °C, the copolymer brush-modified bead packed column exhibited MSC adsorption through hydrophobic interactions between the upper PNIPAAm segment in the copolymer brush and the cells. In addition, the exposed bottom cationic DMAPAAm segment with the shrinking of the PNIPAAm segment enhanced the MSC adsorption, as the MSCs are negatively charged. The optimal amount of PDMAPAAm in the copolymer was determined by changing the composition of the PDMAPAAm segment in the copolymer brush. The PD0.5-*b*-PN brush exhibited effective temperature-modulated MSC adsorption and desorption while maintaining cell viability. Using the PD0.5-*b*-PN column, the separation of MSCs and the BM-CD34⁺ cells was performed. At 37 °C, most of the BM-CD34⁺ cells were eluted from the column, whereas the MSCs were adsorbed on to the column. By reducing the temperature to 4 °C, the adsorbed MSCs were eluted from the column. The differences in the cell adsorption properties on the column at each temperature led to the temperature-modulated separation of the MSCs. In addition, the recovered MSCs from the column maintained their proliferation and differentiation abilities. Thus, the developed column in this study is a useful MSC separation tool, as the MSCs can be simply separated by changing the temperature while maintaining their cellular activity without modifying the cell surfaces.

Conflicts of interest

There are no conflicts of interest to declare.

Acknowledgements

This research was partially supported by a Grant-in-Aid for Scientific Research (grant no. 19H02447 and 20H05233) from the Japan Society for the Promotion of Science and SENTAN (grant no. JPMJSN16B3) from the Japan Science and Technology Agency.

References

- 1 R. Langer and J. Vacanti, *Science*, 1993, **260**, 920–926.
- 2 P. Menasché, A. A. Hagège, M. Scorsin, B. Pouzet, M. Desnos, D. Duboc, K. Schwartz, J.-T. Vilquin and J.-P. Marolleau, *Lancet*, 2001, **357**, 279–280.
- 3 T. Shin'oka, Y. Imai and Y. Ikada, *N. Engl. J. Med.*, 2001, **344**, 532–533.
- 4 K. Nishida, M. Yamato, Y. Hayashida, K. Watanabe, N. Maeda, H. Watanabe, K. Yamamoto, S. Nagai, A. Kikuchi, Y. Tano and T. Okano, *Transplantation*, 2004, **77**, 379–385.
- 5 T. Iwata, M. Yamato, K. Washio, T. Yoshida, Y. Tsumanuma, A. Yamada, S. Onizuka, Y. Izumi, T. Ando, T. Okano and I. Ishikawa, *Regener. Ther.*, 2018, **9**, 38–44.
- 6 M. Sato, M. Yamato, G. Mitani, T. Takagaki, K. Hamahashi, Y. Nakamura, M. Ishihara, R. Matoba, H. Kobayashi, T. Okano, J. Mochida and M. Watanabe, *npj Regener. Med.*, 2019, **4**, 4.
- 7 H. K. Salem and C. Thiemermann, *Stem Cells*, 2010, **28**, 585–596.
- 8 X. Wei, X. Yang, Z.-p. Han, F.-f. Qu, L. Shao and Y.-f. Shi, *Acta Pharmacol. Sin.*, 2013, **34**, 747–754.
- 9 K. Kim, S. Bou-Ghannam, S. Kameishi, M. Oka, D. W. Grainger and T. Okano, *J. Controlled Release*, 2021, **330**, 696–704.
- 10 M. Madrigal, K. S. Rao and N. H. Riordan, *J. Transl. Med.*, 2014, **12**, 260.
- 11 M. Nakao, D. Inanaga, K. Nagase and H. Kanazawa, *Regener. Ther.*, 2019, **11**, 34–40.
- 12 M. Nakao, K. Kim, K. Nagase, D. W. Grainger, H. Kanazawa and T. Okano, *Stem Cell Res. Ther.*, 2019, **10**, 353.
- 13 N. Kaibuchi, T. Iwata, M. Yamato, T. Okano and T. Ando, *Acta Biomater.*, 2016, **42**, 400–410.
- 14 Y. Kato, T. Iwata, S. Morikawa, M. Yamato, T. Okano and Y. Uchigata, *Diabetes*, 2015, **64**, 2723–2734.
- 15 A. Imafuku, M. Oka, Y. Miyabe, S. Sekiya, K. Nitta and T. Shimizu, *Stem Cells Transl. Med.*, 2019, **8**, 1330–1341.
- 16 N. Gandra, D.-D. Wang, Y. Zhu and C. Mao, *Angew. Chem., Int. Ed.*, 2013, **52**, 11278–11281.
- 17 N. Shomali, T. Gharibi, G. Vahedi, R. N. Mohammed, H. Mohammadi, S. Salimifard and F. Marofi, *J. Cell. Physiol.*, 2020, **235**, 4120–4134.
- 18 A. Moldavan, *Science*, 1934, **80**, 188–189.
- 19 L. A. Herzenberg and L. A. Herzenberg, in *Handbook of Experimental Immunology*, ed. D. M. Weir, Blackwell Scientific Publication, Oxford, 1978, ch. 22, pp. 22.21–22.21.
- 20 S. Miltenyi, W. Müller, W. Weichel and A. Radbruch, *Cytometry*, 1990, **11**, 231–238.
- 21 J. C. Giddings, N. Barman Bhajendra and M.-K. Liu, in *Cell Separation Science and Technology*, American Chemical Society, 1991, vol. 464, ch. 9, pp. 128–144.
- 22 K. Kataoka, Y. Sakurai, T. Hanai, A. Maruyama and T. Tsuruta, *Biomaterials*, 1988, **9**, 218–224.
- 23 M. Kamihira and A. Kumar, in *Adv Biochem Engin/ Biotechnol*, ed. A. Kumar, I. Galaev and B. Mattiasson, Springer, Berlin/Heidelberg, 2007, vol. 106, pp. 173–193.
- 24 A. Mahara and T. Yamaoka, *Biomaterials*, 2010, **31**, 4231–4237.



- 25 M. Yamada, W. Seko, T. Yanai, K. Ninomiya and M. Seki, *Lab Chip*, 2017, **17**, 304–314.
- 26 A. Otaka, K. Kitagawa, T. Nakaoki, M. Hirata, K. Fukazawa, K. Ishihara, A. Mahara and T. Yamaoka, *Langmuir*, 2017, **33**, 1576–1582.
- 27 A. Otaka, A. Mahara, K. Ishihara and T. Yamaoka, *J. Micromech. Microeng.*, 2021, **31**, 045012.
- 28 K. Nagase, N. Mukae, A. Kikuchi and T. Okano, *Macromol. Biosci.*, 2012, **12**, 333–340.
- 29 K. Nagase, A. Kimura, T. Shimizu, K. Matsuura, M. Yamato, N. Takeda and T. Okano, *J. Mater. Chem.*, 2012, **22**, 19514–19522.
- 30 K. Nagase, Y. Hatakeyama, T. Shimizu, K. Matsuura, M. Yamato, N. Takeda and T. Okano, *Biomacromolecules*, 2013, **14**, 3423–3433.
- 31 K. Nagase, Y. Sakurada, S. Onizuka, T. Iwata, M. Yamato, N. Takeda and T. Okano, *Acta Biomater.*, 2017, **53**, 81–92.
- 32 K. Nagase, R. Shukuwa, T. Onuma, M. Yamato, N. Takeda and T. Okano, *J. Mater. Chem. B*, 2017, **5**, 5924–5930.
- 33 K. Nagase, R. Shukuwa, H. Takahashi, N. Takeda and T. Okano, *J. Mater. Chem. B*, 2020, **8**, 6017–6026.
- 34 K. Nagase, M. Shimura, R. Shimane, K. Hanaya, S. Yamada, A. M. Akimoto, T. Sugai and H. Kanazawa, *Biomater. Sci.*, 2021, **9**, 663–674.
- 35 M. Nakayama, J. Akimoto and T. Okano, *J. Drug Targeting*, 2014, **22**, 584–599.
- 36 M. K. Jaiswal, M. Gogoi, H. Dev Sarma, R. Banerjee and D. Bahadur, *Biomater. Sci.*, 2014, **2**, 370–380.
- 37 K. Nagase, M. Hasegawa, E. Ayano, Y. Maitani and H. Kanazawa, *Int. J. Mol. Sci.*, 2019, **20**, 430.
- 38 R. Nemoto, K. Fujieda, Y. Hiruta, M. Hishida, E. Ayano, Y. Maitani, K. Nagase and H. Kanazawa, *Colloids Surf., B*, 2019, **176**, 309–316.
- 39 A. Chilkoti, G. Chen, P. S. Stayton and A. S. Hoffman, *Bioconjugate Chem.*, 1994, **5**, 504–507.
- 40 Y. G. Takei, T. Aoki, K. Sanui, N. Ogata, T. Okano and Y. Sakurai, *Bioconjugate Chem.*, 1993, **4**, 42–46.
- 41 J. P. Chen, H. J. Yang and A. S. Hoffman, *Biomaterials*, 1990, **11**, 625–630.
- 42 T. Mori and M. Maeda, *Langmuir*, 2004, **20**, 313–319.
- 43 M. Ebara, J. M. Hoffman, A. S. Hoffman and P. S. Stayton, *Lab Chip*, 2006, **6**, 843–848.
- 44 J. M. Hoffman, P. S. Stayton, A. S. Hoffman and J. J. Lai, *Bioconjugate Chem.*, 2015, **26**, 29–38.
- 45 Y.-J. Kim, S. H. Kim, T. Fujii and Y. T. Matsunaga, *Biomater. Sci.*, 2016, **4**, 953–957.
- 46 M. Matsuura, M. Ohshima, Y. Hiruta, T. Nishimura, K. Nagase and H. Kanazawa, *Int. J. Mol. Sci.*, 2018, **19**, 1646.
- 47 H. Kanazawa, K. Yamamoto, Y. Matsushima, N. Takai, A. Kikuchi, Y. Sakurai and T. Okano, *Anal. Chem.*, 1996, **68**, 100–105.
- 48 K. Nagase and T. Okano, *J. Mater. Chem. B*, 2016, **4**, 6381–6397.
- 49 K. Nagase, S. Kitazawa, S. Yamada, A. M. Akimoto and H. Kanazawa, *Anal. Chim. Acta*, 2020, **1095**, 1–13.
- 50 N. Yamada, T. Okano, H. Sakai, F. Karikusa, Y. Sawasaki and Y. Sakurai, *Makromol. Chem., Rapid Commun.*, 1990, **11**, 571–576.
- 51 Y. Akiyama, A. Kikuchi, M. Yamato and T. Okano, *Langmuir*, 2004, **20**, 5506–5511.
- 52 H. Takahashi, M. Nakayama, M. Yamato and T. Okano, *Biomacromolecules*, 2010, **11**, 1991–1999.
- 53 K. Nagase, M. Watanabe, A. Kikuchi, M. Yamato and T. Okano, *Macromol. Biosci.*, 2011, **11**, 400–409.
- 54 K. Komori, M. Udagawa, M. Shinohara, K. Montagne, T. Tsuru and Y. Sakai, *Biomater. Sci.*, 2013, **1**, 510–518.
- 55 K. Nagase, N. Uchikawa, T. Hirotsu, A. M. Akimoto and H. Kanazawa, *Colloids Surf., B*, 2020, **185**, 110565.
- 56 K. Nagase, Y. Hatakeyama, T. Shimizu, K. Matsuura, M. Yamato, N. Takeda and T. Okano, *Biomacromolecules*, 2015, **16**, 532–540.
- 57 K. Nagase, A. Ota, T. Hirotsu, S. Yamada, A. M. Akimoto and H. Kanazawa, *Macromol. Rapid Commun.*, 2020, **41**, 2000308.
- 58 M. Ciampolini and N. Nardi, *Inorg. Chem.*, 1966, **5**, 41–44.
- 59 K. Okubo, K. Ikeda, A. Oaku, Y. Hiruta, K. Nagase and H. Kanazawa, *J. Chromatogr., A*, 2018, **1568**, 38–48.
- 60 K. Nagase, M. Watanabe, F. Zen and H. Kanazawa, *Anal. Chim. Acta*, 2019, **1079**, 220–229.
- 61 K. Nagase, S. Ishii, K. Ikeda, S. Yamada, D. Ichikawa, A. Akimoto, Y. Hattori and H. Kanazawa, *Sci. Rep.*, 2020, **10**, 11896.
- 62 K. Nagase, Y. Umemoto and H. Kanazawa, *Sci. Rep.*, 2021, **11**, 9976.
- 63 R. F. de Farias and C. Airoidi, *J. Therm. Anal. Calorim.*, 1998, **53**, 751–756.
- 64 K. Nagase, J. Kobayashi, A. Kikuchi, Y. Akiyama, H. Kanazawa and T. Okano, *Langmuir*, 2007, **23**, 9409–9415.
- 65 K. Nagase, J. Kobayashi, A. Kikuchi, Y. Akiyama, H. Kanazawa and T. Okano, *Langmuir*, 2008, **24**, 511–517.
- 66 K. Nagase, A. M. Akimoto, J. Kobayashi, A. Kikuchi, Y. Akiyama, H. Kanazawa and T. Okano, *J. Chromatogr., A*, 2011, **1218**, 8617–8628.
- 67 K. Nagase, J. Kobayashi, A. Kikuchi, Y. Akiyama, H. Kanazawa and T. Okano, *ACS Appl. Mater. Interfaces*, 2012, **4**, 1998–2008.

